EXPERIMENTAL STUDY ON THE THERMAL DAMAGE CHARACTERISTICS OF CEMENT STONE

by

Feng XU [a,b], ***Bowen QIAN*** [b], ***Ling TAN*** [a], ***Jianqiang XU*** [a], ***Shengchuan TANG*** [a], ***Qingyang REN*** [b*], ***and Zhenkun HOU*** [c]

[a] China Merchants Chongqing Communications Research and Design Institute Co., Ltd., Chongqing, China
[b] Chongqing Jiaotong University, Chongqing, China
[c] Guangzhou Institute of Building Science Co., Ltd., Guangzhou, China

Original scientific paper
https://doi.org/10.2298/TSCI200618317X

Aiming at the problem of cement ring sealing failure during deep high temperature shale gas exploitation, comprehensively considering the influence of the characteristics of multi-cluster fracturing of multiple horizontal wells and formation temperature, the cementing cement the southwest region is taken as the research object. After exposure to different temperatures (95 °C and 135 °C) and for different times (5, 10, and 20 times), axial and triaxial tests with different confining pressures (0, 5 MPa, 15 MPa, and 30 MPa) were carried out. The research shows that: the stress-strain curve of cement stone after heat treatment can be divided into four stages: compaction, elastic, yield, and post-peak stage; as the confining pressure increases, the compaction phase disappears, the yield phase increases, and we see the transition from brittle to ideal plasticity after the peak and as the temperature and number of thermal cycles increase, the cohesive force decreases significantly, and the internal friction angle shows a slight increase. The elastic modulus and the peak strength decreased.

Key words: *high temperature cycle, confining pressure, cement stone, strength degradation*

Introduction

As unconventional natural gas, shale gas is mainly composed of methane and is a clean and efficient energy source, which has many types, wide distribution and great potential in China. In recent years, China's shale gas exploration and development, especially in the southwestern region, has made breakthrough progress. From 2016 to 2018, the national shale gas production reached 78.8, 93.0 and 10.88 billion cubic meters, respectively. According to the *Shale Gas Development Plan (2016-2020)* [1], China strives to achieve an annual shale gas output of 30 billion cubic meters in 2020 and 80-100 billion cubic meters in 2030. As a large shale gas resource country, how to transform it into a powerful production country is an urgent need to realize China's energy structure upgrade and low carbon environmental protection strategy.

Deep shale has the characteristics of high temperature, high formation pressure and complex geological conditions. A series of production operations such as perforating, staged fracturing and production require high cementing quality [2, 3], as shown in fig. 1. At pres-

* Corresponding author, e-mail: qyren@cqjtu.edu.cn

ent, more than half of the resources are at a depth of more than 3500 m, in the southwest of China, which is the key shale gas production area. Whether these resources can be effectively developed will affect the development scale of shale gas in China. With the increase of depth, the formation temperature will break through 100 °C, some even exceed 140 °C. In the process of multi-stage fracturing of horizontal wells, the cement sheath is constantly affected by the cyclic alternation of low temperature (fracturing fluid) and high temperature (formation), which can very easily form shear, tensile and interface separation damage [4], resulting in shale gas entering into the cement sheath fracture and generating annular pressure problems [5], as shown in fig. 2. The number of damaged production well is more than 50% at present in Jiaoshiba, Chongqing, which is one of the successful developments of shale gas resources in South China [6, 7]. In Weiyuan shale gas demonstration area, N209, N210, N203, and other wells also have different degrees of annulus pressure phenomena [8]. Generally, the production life of shale gas wells is more than 10 years, which brings serious safety hazards to the safety of the next production. Therefore, how to ensure the integrity of the shale gas well cement sheath under the high temperature environment is a huge challenge for the safe exploitation of shale gas.

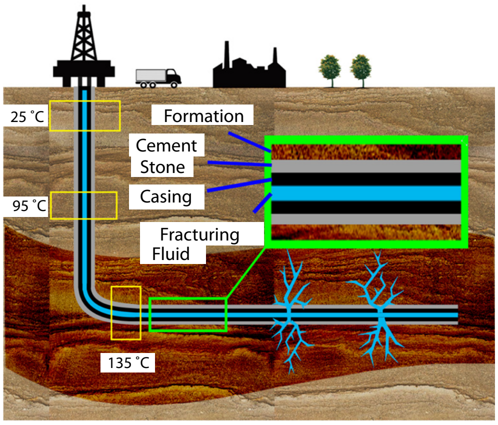

Figure 1. Schematic of the hydraulic fracturing of shale gas

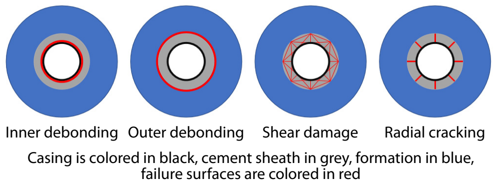

Figure 2. Common failure modes of the cement sheath

Wang *et al.* [9] showed that cement stone exhibits significant elastic-brittleness at room temperature, and its plastic properties increase with increasing temperature, showing approximately linear elasticity-ideal plasticity at 130 °C, and both strength and elastic modulus significantly reduce with increasing temperature. Du *et al.* [10] studied the physical and mechanical properties of cement by micro-indentation tests after cyclic loading and unloading. Their results showed that the hardness and elastic modulus of cement decrease with different degrees after cyclic loading and unloading at high temperatures. Li *et al.* [11] compare the physical and mechanical properties of the normal formulation density of the raw slurry cement stone and the cement stone mixed with 15% latex after curing for 24 hours and 144 hours. Their test results showed that the peak strength of the cement stone after adding latex was increased, and the deformation ability and impact resistance were improved. The cement stone gradually changed from brittle failure to plastic failure with the increase of confining pressure [12]. Zheng *et al.* [13] conducted a comparative study on the mechanical test results of various cement stones (pure cement, elastic, flexible, and ductile cement slurry systems) under different high temperature, confining pressure and loading rate conditions, and then established a relationship between formation temperature and mechanical parameters of cement stone.

The aforementioned scholars have made significant progress in the study of high temperature mechanical properties of cement stone, but in the process of shale gas exploitation, the cement sheath is not in a high temperature state for a long time and is in a dynamic alternating environment. Therefore, it is of great significance to study the physical and mechanical properties of cement stone after it has been affected by cyclic alternating temperature.

Test method

Preparation and processing of samples

Taking the common cement slurry system of shale gas wells in Chongqing as the research object, using G-grade oil well cement and silica fume as the base materials, the formulation of conventional high temperature and high pressure formation conventional cement slurry system with additives such as fluid loss additives, as shown in tab. 1, is selected. We used this cement slurry system to make a 300 mm × 200 mm × 80 mm cube test block and carry out wet curing for 28 days. After curing, we drill, cut and polish according to the standard of petroleum engineering conventional triaxial stress test sample size (Ø25 × 50 mm). The relatively intact cement stone without macrocrack is selected, and the samples with abnormal wave velocity are eliminated on the basis of their longitudinal wave velocity. The standard core of cement stone is shown in fig. 3.

Figure 3. Standard cement specimen

Test method

Thirty six samples of cement stone were selected for this test. All cement stones are heated in an electric heating oven produced by Jiangsu Oven Furnace Manufacturing Co., Ltd., shown in fig. 4. The maximum temperature of the oven is 240 °C, and its accuracy is 1 °C. The rock samples are put in the oven for the thermal-cycling test. The heating speed of the oven is 5 °C per minute. After reaching the target temperature, the temperature is maintained for eight hours, and then the samples are taken out and cooled naturally in the air. To compare the influence of different temperatures of the formation on cement stone, two different temperatures (95 °C and 135 °C) are selected for the thermal-cycle test. The number of thermal cycles is 5, 10, and 20, respectively, according to the field situation of shale gas staged fracturing. The heat-treated specimens were tested by the XTR01-01instrument of the Wuhan Institute of Rock and Soil Mechanics [14], Chinese Academy of Sciences. The maximum confining pressure of the equipment is 80 MPa, the maximum axial load is 200 kN, and the maximum axial displacement is 100.0 mm. The axial de-

Figure 4. High temperature furnace

Table 1. Conventional cement paste formula for high temperature and pressure formations

Name	Compound	Mass fraction [%]
Oil well cement (Class G)	$3CaO \cdot SiO_2$, $2CaO \cdot SiO_2$, 3CaO · Al2O3, $4CaO \cdot Al_2O_3 \cdot Fe_2O_3$, $CaSO_4$	54.6
Silica powder	SiO_2	19.1
Tap water	H_2O	23.0
DZJ-Y (Fluid loss additive)	–	3.3

formation range is 20.0 mm, and the circumferential deformation range is 7.0 mm. The maximum relative error is less than 1.0%. In the test, the confining pressure is first increased to a predetermined value at a rate of 0.5 MPa/s, and the confining pressure is kept constant. Then, the axial load is applied to the failure or a certain displacement value with a displacement control of 0.18 mm per minute.

Test results and analysis

Characteristics of the stress-strain curves

The triaxial stress-strain curves of cement stones treated with different high temperatures and thermal cycles are shown in fig. 5. Under different confining pressures, the stress-strain curve can be divided into four stages: compaction stage, elastic stage, yield stage and post-peak stage:

- *Initial compaction stage*: This stage is very obvious under uniaxial conditions, and has an obvious closing period under the axial load, which indicates that cement stone is a porous material after high temperature cycling. In the triaxial tests, the compaction stage is not so obvious because the pores and microcracks have been compacted under the confining pressure.
- *Elastic stage:* as the axial load increases, the stress-strain curve quickly enters the linear elastic stage and the slope of the curve remains unchanged. Generally, the larger the confining pressure, the longer the linear elastic stage is.
- *Yield stage:* in the uniaxial test, the trend of slope decrease is not obvious, which can be ignored. In the triaxial test, as the axial load gradually increases, the upward trend of the stress-strain curve gradually becomes slower. As the confining pressure increases, the yield characteristics of the cement stone become more obvious, and the yield stage is also clearer. The mechanical properties of cement stone are transformed from brittleness to plasticity with confining pressure increasing.
- *Post-peak stage*: when the axial stress reaches the peak stress under the uniaxial condition, the microcracks quickly develop into macrocracks, and the samples lose their bearing capacity without residual strength. At a confining pressure of 5 MPa, when the stress reaches the peak stress, the microcracks gradually merge and form a macro-shear crack. Due to the small confining pressure, the curve has an obvious fall and a slow downward trend. At a confining pressure of 15 MPa, when the stress reaches the peak stress, the curve has a slight drop to maintain as tab. stress value. When the confining pressure reaches 30 MPa, the curve has no obvious peak, and the stress remains unchanged after the yield stage because the large confining pressure limits the penetration of the crack and the stress does not fall.

Change of physical and mechanical parameters

- Peak strength

As shown in figs. 5 and 6 and tab. 2, the peak strength of samples S021, S027, and S033 after 5, 10, and 20 times of thermal cycling at 95 °C is 76.28, 71.78, and 65.56 MPa,

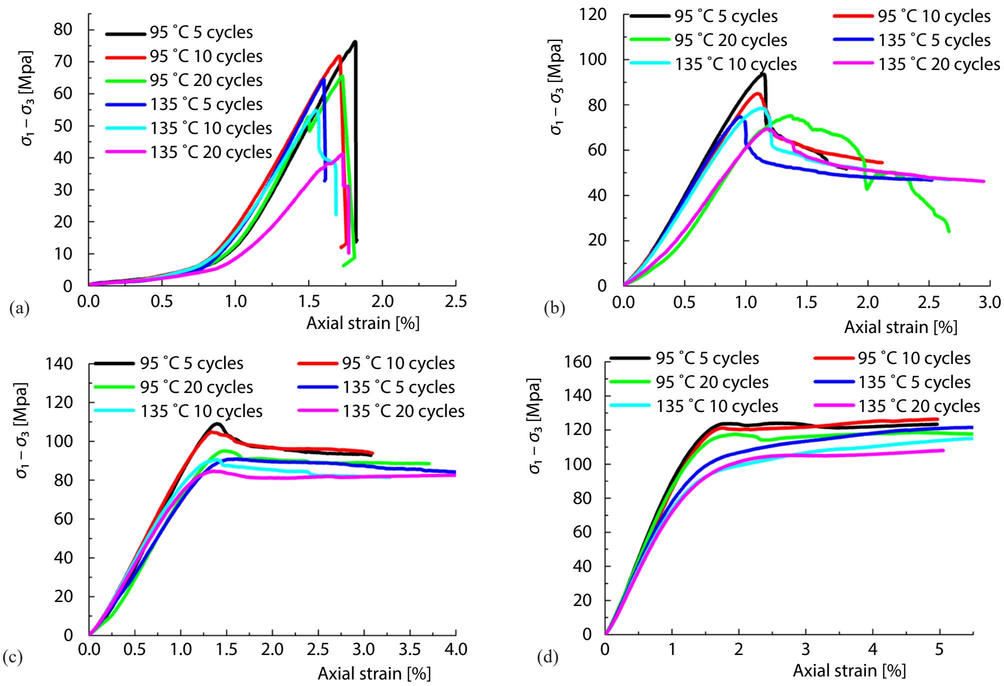

Figure 5. Stress-strain curves of cement after high temperature cycling; (a) 0 MPa, (b) 5 MPa, (c) 15 MPa, and (d) 30 MPa

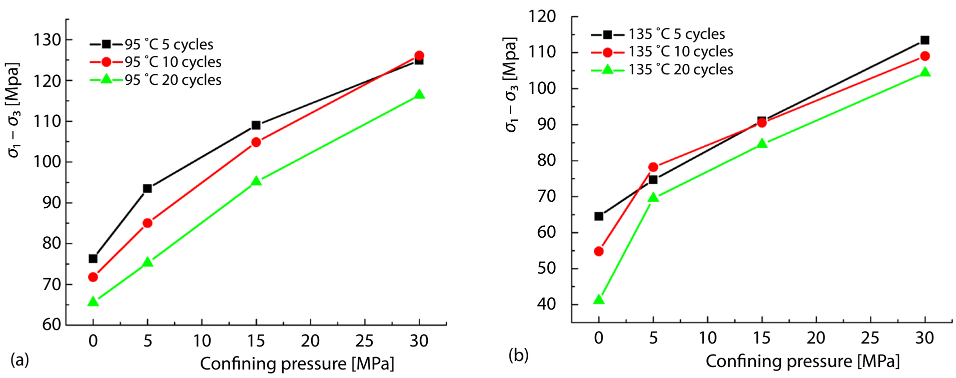

Figure 6. Relationships between peak strength and confining pressure after high temperature cycling; (a) 95 °C and (b) 135 °C

respectively, while that of samples S039, S045, and S051 after 5, 10, and 20 times of thermal cycling at 135 °C is 64.53, 54.80, and 41.13 MPa, respectively. Under the same cycle times, the reduction rate of the peak strength after 135 °C thermal cycle treatment was 15.4%, 23.7%, and 37.2% of the peak strength after 95 °C thermal cycle treatment, indicating that under the same thermal cycle times, as the thermal cycle temperature increases the more serious the internal damage of the cement stone and the more obvious the uniaxial peak strength decreases.

In the same way, the triaxial peak strength and the uniaxial peak strength have the same trend. As a whole, as the number of thermal cycles and the temperature of the thermal

Table 2. Strength parameters of cement stone after treatment with different temperatures and cycle times

	Specimen number	Density after heat treatment	Confining pressure [MPa]	Peak strength, $\sigma_1 - \sigma_3$ [MPa]	Elastic modulus [GPa]	Cohesion, c [MPa]	Internal friction angle, φ [°]
95 °C 5 cycles	S021	1.71	0	76.28	8.42	25.71	25.69
	S022	1.69	5	93.49	9.65		
	S023	1.67	15	109.00	9.59		
	S024	1.65	30	124.89	9.72		
95 °C 10 cycles	S027	1.71	0	71.78	8.14	22.41	28.07
	S028	1.61	5	85.03	8.95		
	S029	1.63	15	104.86	9.23		
	S030	1.65	30	126.07	9.44		
95 °C 20 cycles	S033	1.67	0	65.56	8.62	20.36	27.31
	S034	1.68	5	75.25	8.06		
	S035	1.68	15	95.08	8.62		
	S036	1.68	30	116.36	9.11		
135 °C 5 cycles	S039	1.69	0	64.53	8.06	20.35	26.50
	S040	1.69	5	74.68	9.08		
	S041	1.71	15	91.02	7.65		
	S042	1.64	30	113.44	8.28		
135 °C 10 cycles	S045	1.70	0	54.80	7.10	19.24	26.82
	S046	1.62	5	78.18	8.58		
	S047	1.65	15	90.50	8.24		
	S048	1.69	30	109.04	7.67		
135 °C 20 cycles	S051	1.67	0	41.13	5.26	14.96	29.23
	S052	1.66	5	69.49	7.51		
	S053	1.64	15	84.51	7.92		
	S054	1.71	30	104.33	7.58		

cycles increases, the triaxial peak strength decreases. When the confining pressure is 5 MPa, the peak strength of sample S022 after five thermal cycles at 95 °C is 93.49 MPa, while the peak strength of sample S052 after 20 thermal cycles at 135 °C is 69.49 MPa, and the strength reduction is 25.7%. When the confining pressure is 15 MPa, the peak strength of S023 after five times of thermal cycling at 95 °C is 109.00 MPa, while that of S053 after 20 times of thermal cycling at 135 °C is 84.51 MPa, and the strength reduction rate is 22.5%. When the confining pressure is 30 MPa, the peak strength of S024 after five times of thermal cycling at 95 ℃ is 124.89 MPa, while that of the piece S054 after 20 times of thermal cycling at 135 ℃ is 104.33 MPa, and the strength reduction rate is 16.5%.

– Elastic modulus

Under different confining pressures, the change trend of the elastic modulus is approximately the same: it decrease with the increase of temperature and the number of cycles. For example, in uniaxial compression, the modulus of elasticity of sample S021 after five thermal cycles at 95°C is 8.42 GPa. The elastic modulus of S051 after 20 cycles of 135 °C is only 5.26 GPa, and the elastic modulus reduction is 37.5%. The modulus of elasticity under triaxial compression and the modulus of elasticity under uniaxial have the same tendency. The elastic modulus of sample S022 at a confining pressure of 5 MPa after five thermal cycles at 95 °C is 9.65 GPa. The elastic modulus of S052 with 20 thermal cycles was 7.51 GPa, and the reduction of the elastic modulus is 22.2%.

– Cohesion and internal friction angle

Based on the *Mohr-Coulomb* failure criterion, the cohesion and internal friction angle of cement stones are calculated. It can be seen from tab. 3 that the internal friction angles of cement stones with different heat treatments are 25.69°, 28.07°, 27.31°, 26.50°, 26.82°, and 29.23°, respectively. As the number of thermal cycles and the temperature of the thermal cycle increase, the internal friction angle shows a slight increase. The cohesion of cement stone decreases gradually from 5 to 20 thermal cycles at different temperatures, from 25.71-20.36 MPa at 95 °C, with a reduction of 20.8%, from 20.35-14.96 MPa at 135 °C, a reduction of 26.5%, indicating that the cohesion of cement stone decreases obviously with the increase of the number of cycles. At the same number of cycles of 5, 10, and 20, the cohesion at 135 °C decreased by 20.8%, 14.1%, and 26.5%, respectively, compared with 95 °C, indicating that the cohesion of cement stones decreased significantly with the increase of cycling temperature.

Table 3. Cohesion and internal friction angle of cement after high temperature cycling

Heat treatment method	Linear fitting formula $y = ax + b$	a mean value	b mean value	Internal friction angle, φ [°]	Cohesion, c [MP]
95 °C 5 cycles	$y = 2.53x + 81.79$	2.53	81.79	25.69	25.71
95 °C 10 cycles	$y = 2.78x + 74.71$	2.78	74.71	28.07	22.41
95 °C 20 cycles	$y = 2.70x + 66.87$	2.70	66.87	27.31	20.36
135 °C 5 cycles	$y = 2.61x + 65.77$	2.61	65.77	26.50	20.35
135 °C 10 cycles	$y = 2.64x + 62.58$	2.64	62.58	26.82	19.24
135 °C 20 cycles	$y = 2.91x + 51.01$	2.91	51.01	29.23	14.96

Analysis of temperature influence mechanism

When the cement stone is thermally cycled in the temperature range of 95 °C or 135 °C, due to the different thermal expansion coefficients of different mineral components of the cement stone, the mineral particles repeatedly expand and contract unevenly, resulting in differential deformation between the mineral components. As the number of cycles increases, the deformation becomes more serious, resulting in the accumulation of microcracks between mineral components, which eventually results in the decrease in the cohesion of cement stone. Simultaneously, the high temperature at 135 °C is more likely to cause the expansion and contraction of cement stone than the 95 °C, and the damage is more serious at the 135 °C thermal cycle. However, during the high temperature cycle, the free water and bound water in the mineral composition volatilize, which causes the surface to become rougher and then the internal friction angle shows a slight increase as the thermal cycle temperature and the number of thermal cycles increase.

After the action of the high temperature cycle, the microscopic damage of cement stone is manifested by the weakening of mechanical parameters such as peak strength and elastic modulus. For a particular solid material, as the internal damage increases, the cohesive force decreases, the ability of the material to resist deformation decreases, and the macroscopic performance will be a reduction in elastic modulus. Therefore, as the temperature and number of thermal cycles increase, the elastic modulus of cement stone decreases significantly. The peak strength is mainly affected by cohesion and internal friction angle. Although the internal friction angle increases slightly with the increase of thermal cycle temperature and number of cycles, it is not enough to make up for the strength damage caused by loss of cohesion, so the ultimate manifestation is a decrease in peak strength.

Conclusions

- The stress-strain curve of cement stone after heat treatment is divided into four stages: compaction stage, elastic stage, yield stage, and post-peak stage. As the confining pressure increases, the compaction phase disappears, the yield phase increases and the peak transitions from brittleness to ideal plasticity.
- With the increase of the temperature and the number of thermal cycles, the cohesive force showed a significant decrease, the internal friction angle showed a slight increase, and the macroscopic behavior showed a decrease in both the elastic modulus and peak strength.

Acknowledgment

The authors would like to acknowledge professor J. J. K. Daemen at the University of Nevada, USA, for his English help, and the financial support of the National Key Research and Development Program of China (2018YFC1504903), Chongqing postdoctoral science foundation Grant (cstc2020jcyj-bshX0021), China postdoctoral science foundation Grant (2019M662918) and Regional Joint Fund for Basic and Applied Basic Research Fund of Guangdong Province (2019A1515110836).

Nomenclature

c – cohesion, [MPa]

Greek symbols

σ_1 – maximum principal stress, [MPa]
σ_3 – minimum principal stress, [MPa]
φ – internal friction angle, [°]

References

[1] ***, National Energy Administration, Shale Gas Development Plan (2016-2020), Beijing, China, 2016
[2] Xia, Y. B., *et al.*, Analysis of the Technical Difficulties of Shale Gas Well Cementing (in Chinese), *Natural Gas Exploration and Development*, *39* (2016), 1, pp. 74-76
[3] Xu, F., *et al.*, Effect of the Drilling Fluid on Hardness Characteristics of Tight Sandstone, *Current Science*, *115* (2018), 11, pp. 2015-2018
[4] Qi, F. Z., *et al.*, Analysis of Causes of Gas Well Annulus Pressure and Solutions (in Chinese), *Meeting of Directors of Petroleum Drilling Institute*, (2008), pp. 802-806
[5] Saint-Marc, J., *et al.*, Initial State of Stress: The Key to Achieving Long-Term Cement-Sheath Integrity, *Proceedings*, SPE Annual Technical Conference and Exhibition, Society of Petroleum Engineers, Denver, Col., USA, 2008
[6] Sun, K. Zh., *et al.*, Cementing Technology for Deep Shale Gas Horizontal Well in the Dingshan Block, *Petroleum Drilling Techniques*, *43* (2015), 3, pp. 55-60
[7] Xu, F., *et al.*, Effect of Bedding Planes on Wave Velocity and AE Characteristics of the Longmaxi Shale in China, *Arabian Journal of Geosciences*, *10* (2017), 6, pp. 1-10
[8] Tao, Q., Chen, X. X., Causal Analysis and Countermeasures on B Sustained Casing Pressure of Shale-Gas Horizontal Wells in the Sichuan Basin (in Chinese), *Oil Drilling and Production Technology, 39* (2017), 5, pp. 588-593
[9] Wang, L., *et al.*, Experimental Study on Mechanical Properties of Oil Well Cement under High Temperature (in Chinese), *Journal of China University of Petroleum (Edition of Natural Science)*, *42* (2018), 6, pp. 93-100

[10] Du, H., *et al*., *Microstructure and Micromechanics of Wellbore Cements under Compression and Thermal Loading*, American Rock Mechanics Association, Alexandria, Va., USA 2015
[11] Li, Z. Y., *et al*., Improvement of Latex on Mechanical Deformation Capability of Cement Sheath under Triaxial Loading Condition (in Chinese), *Acta Petrolei Sinica*, *28* (2007), 4, pp. 126-129
[12] Li, Z. Y., *et al*., Deformation Behavior of Oil-Well Cement Stone under Confining Pressure (in Chinese), *Natural Gas Industry*, *27* (2007), 9, pp. 62-64
[13] Zheng, Y. Z., *et al*., Mechanical Behaviors of Cement Systems in Different Conditions (in Chinese), *Natural Gas Industry*, *37* (2017), 1, pp. 119-123
[14] Xu, F., *et al*., Effect of Confining Pressure on the Mechanical Properties of Thermally Treated Sandstone, Current science, *112* (2017), 6, pp. 1101-1106

Paper submitted: June 18, 2020
Paper revised: September 6, 2020
Paper accepted: September 27, 2020